Controlling Quantum Pathways in Molecular Vibrational Polaritons

Zimo Yang[1], Bo Xiang[1], Wei Xiong[1,2]

[1]Materials Science and Engineering Program, UC San Diego, La Jolla, CA

[2]Department of Chemistry and Biochemistry, UC San Diego, La Jolla, CA

Abstract

Molecular vibrational polaritons, hybrid quasi-particles formed by molecular vibrations and cavity photons through strong light-matter coupling, have attracted much attention due to their potential to alter photonic properties and to change the course of chemical reactions. The ultrafast dynamics of molecular vibrational polaritons have been studied to advance our understanding of these interesting hybrid quasiparticles. For example, the roles of dark states, hot vibrational mode relaxation in cavities, and manipulation of nonlinear interactions have been investigated by ultrafast spectroscopy. However, the coherent nature of polaritons makes many viable quantum pathways able to contribute to 2D IR spectral signals, complicating its interpretation. Here, using a mid-IR pulse shaper, we report an experimental way to directly measure polariton nonlinear responses involving specific quantum pathways by eliminating others. For example, either coherence or population states may be exclusively probed. This work is useful for the development

of polariton based quantum technologies, research into the role of coherence in energy transportation in artificial and natural energy materials, and cavity chemistry.

Keywords

Molecular vibrational polariton; two-dimensional infrared spectroscopy; Feynman diagrams; ultrafast dynamics; strong coupling; microcavity

Introduction

Strong coupling between molecular vibrational and microcavity electromagnetic modes leads to delocalized superpositions of these modes, which result in molecular vibrational polaritons[1–6]. Heuristically, polaritons arise when a cavity photon interconnects the microscopic molecular degrees of freedom[1–8], rendering the eigenstates of the system described as the hybridization of both modes. Two new bright hybrid eigenstates are formed with their characteristic transition frequencies. The lower frequency eigenstate is known as the lower polariton (LP) while the other, at a higher frequency, is known as the upper polariton (UP) (Figure 1a). Molecular vibrational polaritons have shown many unique and promising features for photonics and chemistry. For example, we have demonstrated strong coupling allows optical nonlinearity of polaritons to be controlled through macroscopic parameters such as cavity longitudinal length and molecular concentrations[9]. Furthermore, the Ebbesen group has recently demonstrated the altering of chemical selectivity of reactions when reactants are strongly-coupled to cavities[10–14]. Aside from these promising developments, there have been other novel phenomena being proposed for molecular vibrational polaritons, e.g. room-temperature realizations of superfluids, polariton lasing, and polariton condensates.

These developments and the potential of molecular vibrational polaritons motivate us[9,15–17] and Owrutsky, Dunkelberger and others[6,18] to pursue the understanding and manipulation of vibrational polariton states from the aspect of their fundamental dynamics, by employing ultrafast IR pump-probe and 2D IR spectroscopy[9,15,16,19–21] (Figure 1b). Using 2D IR spectroscopy, we have successfully resolved quantum states in polaritons, mechanisms of energy transfer between polaritons, and hidden dark reservoir states[9,15,16]. While 2D IR spectroscopy can resolve signals from different quantum states to a certain degree, each spectral signal still has contributions from

different quantum pathways. Although some of these pathways could be distinguished and analyzed by phase-matching and post-analysis[9,22], it would be useful to selectively excite specific quantum states to understand the evolution of particular pathways of interest. For example, to differentiate a certain physical process, e.g. energy transfer, whether it is initiated from population or coherence states, it is more straightforward to create these directly, to avoid any interference from other pathways.

In this letter, we report a pulse-shaper based method[23–25] to selectively excite specific quantum pathways in 2D IR measurements and realize the preparation of selective coherence and population states. We verify that the desired quantum states are excited, and quantify the dynamics associated with them. These developments represent a major step forward in controlling quantum states in polaritons for the development of mid-IR photonic nonlinear devices and quantum information systems.

Results

The polariton sample is prepared by sandwiching a saturated $W(CO)_6$ solution in a microcavity composed of two DBR windows separated by a 25-um spacer[15] (Fig.1d). In the strong coupling regime, UP and LP are formed upon the hybridization of vibrational and cavity modes (Fig.1a).

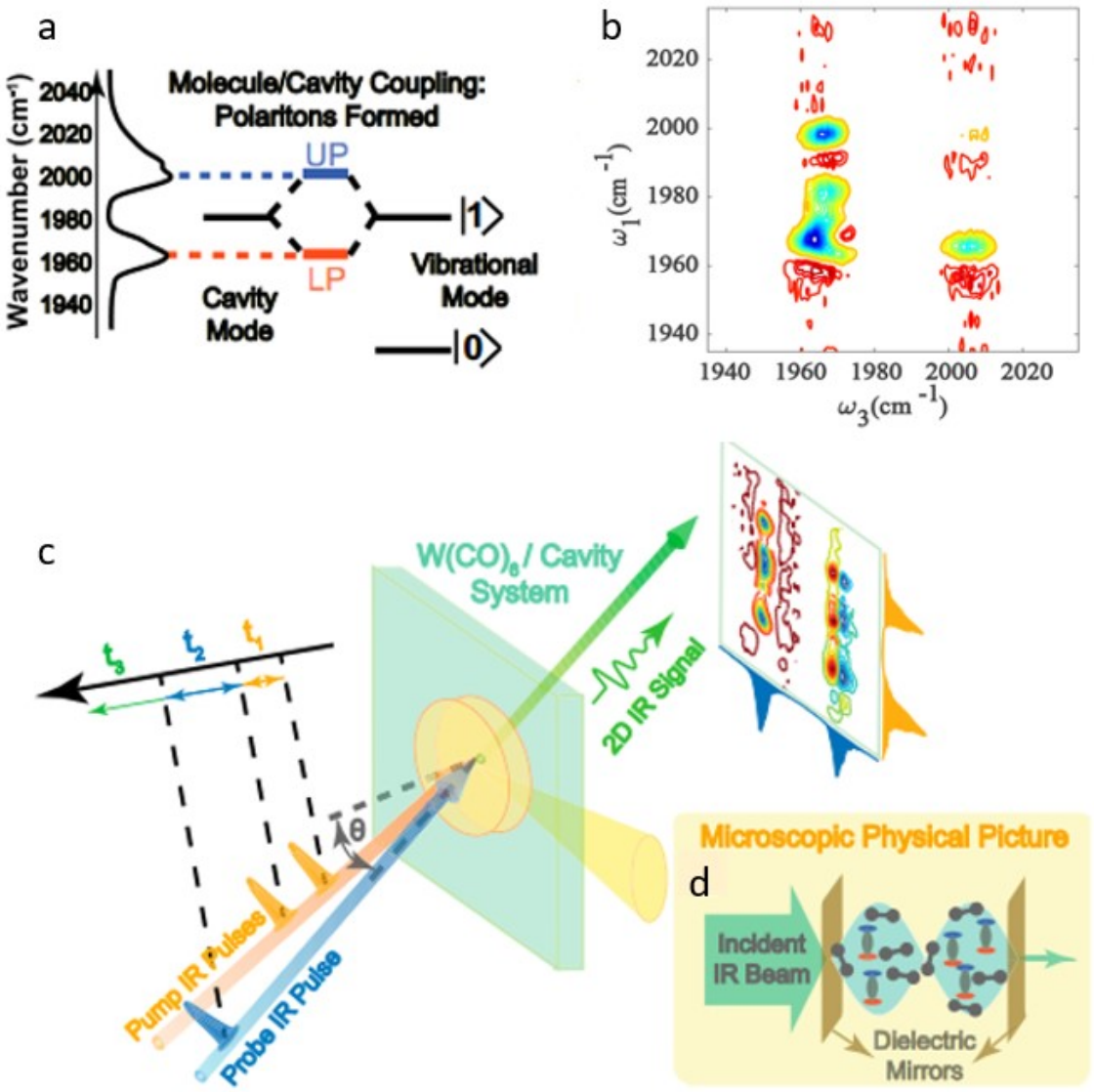

Figure 1. Vibrational polariton 2D IR spectroscopy. (a) Formation of vibrational polaritons by strongly coupled molecular vibration and cavity modes. (Left) the vibrational polariton FTIR spectrum of $W(CO)_6$. (b)Two-dimensional IR spectrum of $W(CO)_6$/cavity–polariton system at 0-ps delay. Color map: red is positive, blue is negative. (c) Scheme of vibrational polariton 2D IR spectroscopy setup. Pump and probe IR incident beams are symmetric with respect to the normal plane with the same tilting angle, θ. The coherences are characterized by scanning t_1 and t_3, and

the resulting time-domain interferograms are Fourier transformed to obtain 2D IR spectra. The other delay time, t_2, is equivalent to the delay between the pump and probe pulses in pump-probe spectroscopy. (d) Illustration of the microscopic physics of molecules inside of a microcavity where "pure gray modes" correspond to the vibrational modes that are not strongly coupled to the cavity and the rest refers to the strongly coupled modes that contribute to UP (blue), LP (red), and dark reservoir modes (gray) formation.

Two-Dimensional IR Spectra of Vibrational Polaritons and their Feynman Diagrams. To obtain 2D IR spectra, we use pump-probe geometry to measure the transient absorption spectra as a function of t_1 (Fig.1c). Then, a 2D IR spectrum is generated numerically by Fourier transform of the t_1 free induction decay (FID) at individual probe (ω_3) frequency. An example 2D IR spectra of molecular vibrational polaritons is shown in Figure 1b. Details of analysis about 2D IR spectra of this polariton system have been reported in our previous work[9,15,16]. Briefly, at early t_2 delay, the peaks at diagonal represents interactions between the same polariton states, whereas the cross peaks indicate interactions between UP and LP[9]. At longer t_2 delay, when polaritons relax to dark modes, Rabi splitting contraction dominate the signals and usually, an overtone transition of the dark mode appears near LP frequency[4,6,15]. Nevertheless, each peak still is a superposition of signals from several quantum pathways of the polaritons. If we don't consider double quanta coherence, which emits at a different phase-matching direction, at early t_2 delays, there are a total of 30 quantum pathways, illustrated as double-sided Feynman Diagrams[26] (Figure 2), that contribute to all polariton spectral peaks.

To discuss their utility, a brief overview of double-sided Feynman diagrams is given here. A double-sided Feynman diagram is a pictorial representation of a nonlinear response function[26]. From bottom to top, the arrows represent weak light-matter interactions as a function of time,

where the pointed-in/out arrows represent creation and annihilation operators, respectively. As a third-order nonlinear signal, in total, it has three light-matter interactions before the final emission (last curly arrow). The waiting period between arrows is the evolution times of coherence or population states after light-matter interactions. For example, in A3, the first excitation created a coherence |UP><0| state, and after letting this state evolve over t_1 time delay, the second pulse transfer the initial |UP><0| state into a |UP><UP| population state, which evolves during t_2, before it is excited to |UP+LP><UP| coherence by the third pulse. A macroscopic polarization then freely evolves in t_3 and emits an FID signal for detection.

Figure 2 shows that there are many quantum pathways can contribute to 2D IR signals. Some of them can be differentiated because they have different dynamics. For example, while the systems are always in coherence states during t_1 and t_3, during t_2, it can either involve coherence or population states, which leads to distinguishable t_2 dynamics. When a population state is created, the dynamics occurring during t_2 represents population relaxation and when a coherence state is involved, the dynamics should manifest as an oscillation[9,22]. In our previous work, we have used the dynamical differences during t_2 to numerically separate these quantum paths, by applying Fourier filters[9,22]. However, a t_2 scan is a necessity to differentiate them. In this work, using a pulse shaper, we show a method to directly excite selective quantum pathways without the involvement of scanning t_2. Such a method could be useful in quantum information technology when only tailored quantum states are needed, and in fundamental research when the contributions from coherence and population states need to be differentiated.

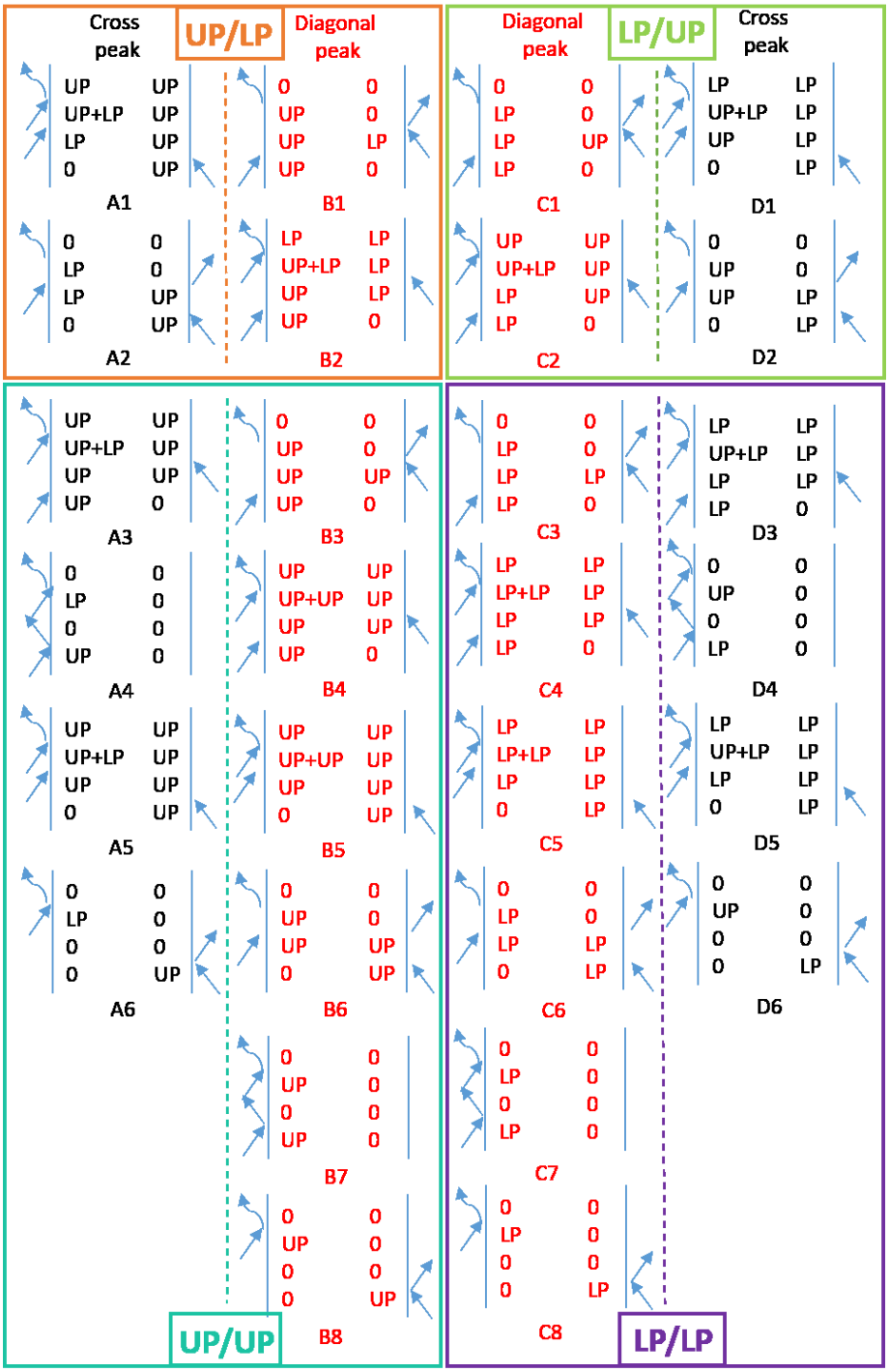

Figure 2. Feynman diagrams of all quantum pathways in 2D IR measurements of polaritons. The (UP/UP), (LP/UP), (UP/LP) and (LP/LP) subgroup pathways can be prepared by pulse sequence (a) to (d) in Figure 3, respectively.

Tailored pulse sequence for quantum pathway-specific 2D IR spectrum. Multiple quantum pathways contribute to the same 2D IR spectra because the pump pulse pairs used in 2D IR are broadband and contain two Gaussian pulses in the time domain, each of which has full spectral coverage (Figure 3e). Thus, UP and LP states are simultaneously excited.

To preferentially excite only a subset of them, we tailor the spectra of a pump pulse pair, using the mid-IR pulse shaper[24]. We program the arbitrary waveform generator (AWG) to shape and generate the double pulse pair using a Germanium (Ge) based Acoustic Optical Modulator (AOM). We can preferentially engineer both pulses to only possess half of the spectral coverage. For example, a pulse may be generated composed of the spectral component to excite only |LP>, which leads to a |LP><LP| population state (Figure 3d), or having the first and second pulse covering complementary spectral ranges to first excite |UP> and then |LP>, to create a |LP><UP| or |UP><LP| coherence (e.g. Figure 3c). There are totally 4 different combinations for the tailored pump pulse pairs, summarized in Figure 3.

Each tailored pulse sequence would enable signals from a subset of Feynman diagrams, which allows the entire 30 Feynman diagrams to be separated in four groups. We labeled these four groups in Figure 2, based on their first two light-matter interactions. For example, the label (UP/UP) in Figure 2 indicates when the pulse sequence (UP/UP) of Figure 3a is used, the first interactions excite |UP> (or <UP|), while the second interactions involve |UP> (or <UP|). As a result, only signals involving Feynman diagram A3-A6, and B3-B8 should be created when tailored pulse sequence (UP/UP) of Figure 3a is applied.

Feynman pathways that are excited by the same tailored pulse sequence can be further distinguished because they appear at different spectral locations. For example, A3-A6 should appear at $\omega_1 = \omega_{UP}$ and $\omega_3 = \omega_{LP}$, as a cross-peak whereas B3-B8 $\omega_1 = \omega_{UP}$ and $\omega_3 = \omega_{UP}$, as a

diagonal peak. Thus, by applying these tailored pulse sequences, the 30 different pathways should be break into many subgroups based on their dependence on the tailored pulse sequences and their spectral locations.

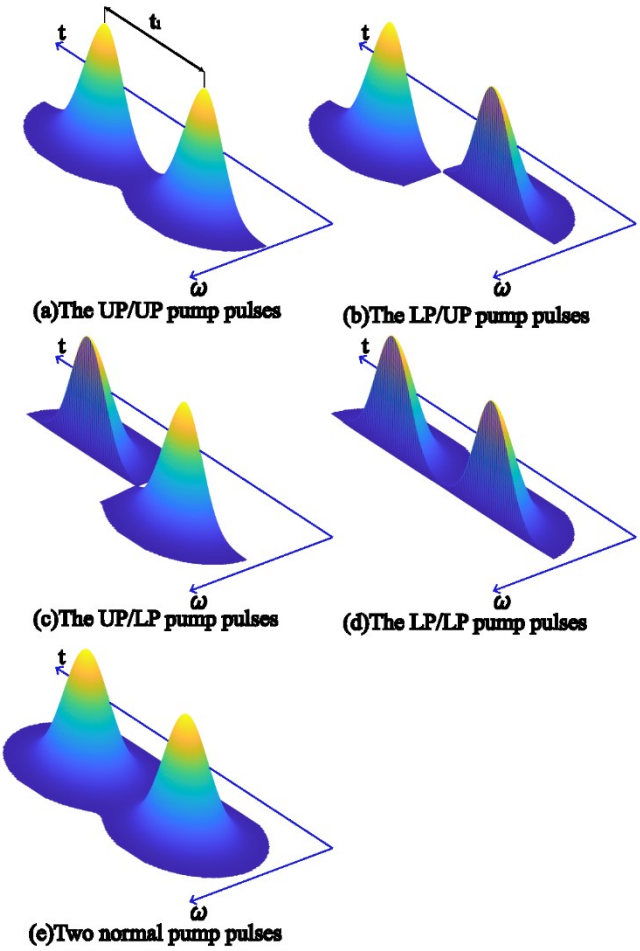

Figure 3 Tailored two half-Gaussian pump pulses. (a) UP/UP pulse, both first and second pulses only excite UP states, (b) LP/UP pulse, first and second pulses excite LP and UP, respectively, (c) UP/LP pulse, first and second pulses excite UP and LP, respectively, (d) LP/LP pulse, both first and second pulses only excite LP states, (e) broadband pump pulse pairs.

To examine this idea, we acquired 2D IR spectra using the tailored pulse sequences. When UP/UP pulse sequence is used, only two peaks at $\omega_1 = \omega_{UP}$ appear, a diagonal peak and a cross peak corresponding to B3-B8 and A3-A6, respectively (Figure 4a). This is expected because LP

is not involved in this pump pulse sequence – all peaks at $\omega_1 = \omega_{LP}$ are missing. When the UP/LP pulse sequence is applied, two peaks also appear at the same $\omega_1 = \omega_{UP}$ position (Figure 4b, where the dispersive line-shape along ω_1 is due to uncertainty in setting $t_2 = 0$ fs.). The UP/UP and UP/LP pulse sequences result in peaks at the same position, because the first pulse excites |UP> in both cases. However, they involve different states during t_2, as we describe in the next section. Indeed, there are some line-shape differences between peaks in Figures 4a and b because the two spectra experience different quantum pathways: Figure 4a involves population states during t_2 and the corresponding spectral signatures are Rabi splitting contraction and excited state absorption of dark modes[4,6,15]. In contrast, Figure 4b involves coherence during t_2, which causes decoherence accelerations and an absorptive transient feature we refer to as polariton bleach[9]. Thus, the subtle spectral differences already encode the different quantum pathways involved in different pulse sequences. Similarly, if LP/LP or LP/UP pulse sequences are used, the spectra feature only show up at $\omega_1 = \omega_{LP}$ (Figure 4 c and d). We note the conventional out-of-phase "overtone" peak is missing. This is due to the mechanical anharmonicity of either overtone or combination bands of polaritons being small. Instead, the oscillator strength of overtone/combinational bands deviates from the harmonic oscillator model, which does not completely cancel the fundamental band signal, results in nonlinear signals[9].

Ideally, each of the four spectra resulted from the tailored pulse sequences represents a subset of the quantum pathways when broadband pulse sequences (Figure 3e) are used. Thus, when the four spectra are numerically summed together, the resulting spectra (Figure 4e) should reproduce the 2D IR spectra taken using broadband pulse sequences (Figure 4f). This is indeed the case, as the two spectra resemble each other, validating the fidelity of our method.

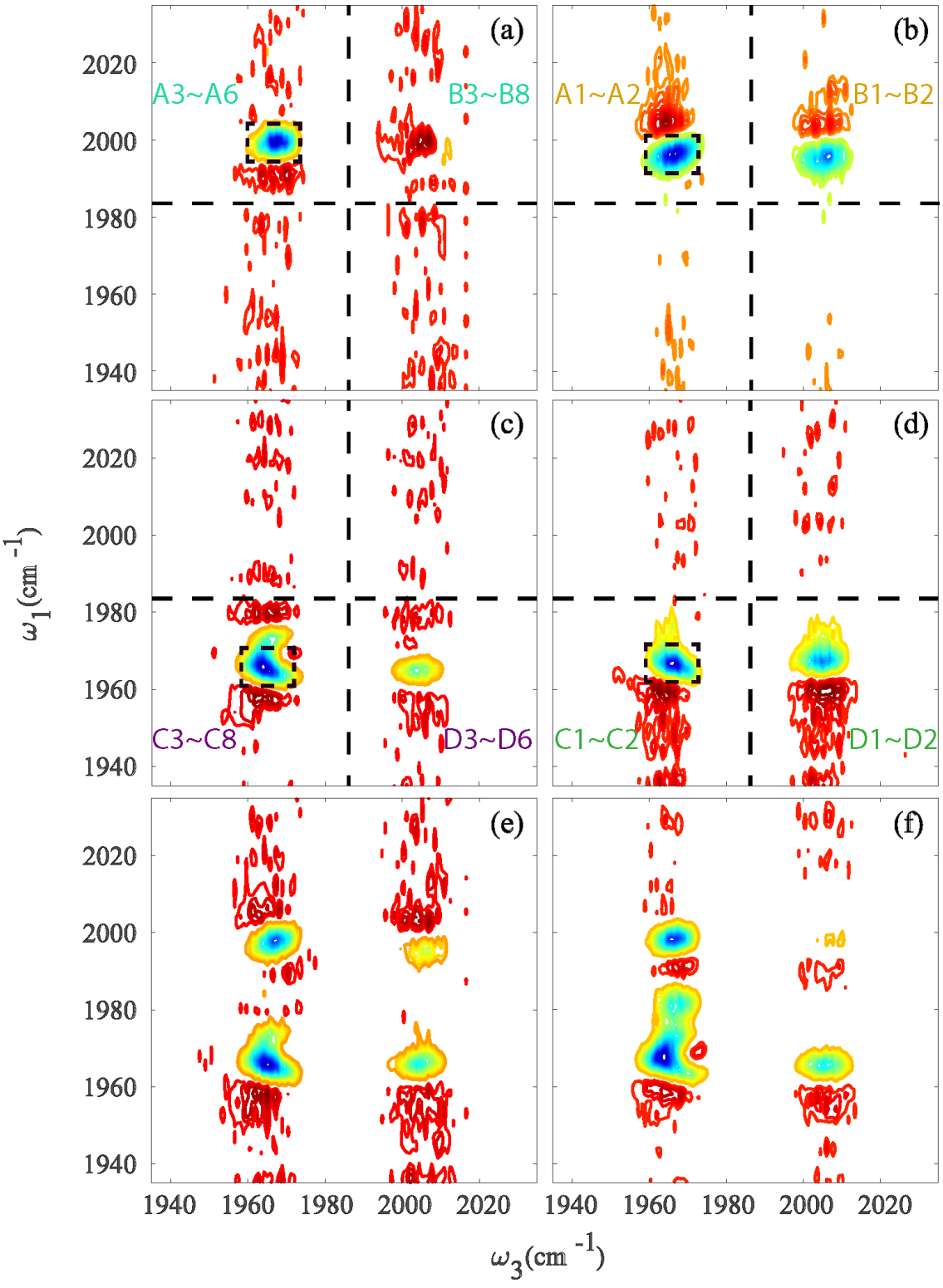
(a)
(b)
(c)
(d)
(e)
(f)
A3~A6
B3~B8
A1~A2
B1~B2
C3~C8
D3~D6
C1~C2
D1~D2
2020
2000
1980
1960
1940
ω_1(cm^{-1})
ω_3(cm^{-1})

Figure 4 Two-dimensional IR spectrum of $W(CO)_6$/cavity-polariton system with two tailored pump pulses only containing (a) (UP/UP) (b) (UP/LP) (c) (LP/LP) (d) (LP/UP) corresponded frequency component individually; (e) Summation of (a) to (d) is qualitatively similar to (f) the 2D IR spectrum of a polariton system pumped by two broadband pump pulses. All 2D IR spectra are taken at t_2 = 0 ps. Peaks in (a)~(d) are labeled by the indices in Feynman diagrams in Fig.2.

Dynamics of different quantum pathways. The four 2D IR spectra in Figure 4 a-d, demonstrate we can separate signals involving |LP><0| (or |0><LP|) and |UP><0| (or |0><UP|) during t_1. Yet, all four spectra indeed involve different quantum pathways – spectra in Figures 4a and c, and Figures 4b and d involve population and coherence state during t_2, respectively. Thus, they should exhibit different dynamics during t_2. To see it, we acquire 2D IR spectra as a function of t_2, using the tailored pulse sequences. Then, the integrated pixel intensity (labeled by dashed rectangular boxes in Figure 4) is plotted as a function of t_2.

Figure 5 shows that the dynamic traces of polaritons pumped by all four tailored pump pulse sequences exhibit different time-dependent behaviors. When (UP/UP) pulse sequence is applied, a population relaxation dynamics is observed (Figure 5a), while when (UP/LP) pulse sequence is used, a dynamic oscillating at a period of 800 fs, corresponding to 41.7 cm^{-1} appears (Figure 5b), whose frequency also agree with the Rabi splitting. This dynamic difference reveals the different quantum pathway prepared by (UP/UP) and (UP/LP) pulse sequences. Despite that pulse sequences (UP/UP) and (UP/LP) both excite the same coherences by the first pulse, generating similar 2D IR spectra, the second of the light-matter interaction yields completely different dynamics: during t_2, (UP/UP) pulse sequence generates |UP><UP| population states, leading into a population relaxation decay of the systems (Figure 5a), whereas pulse sequence (UP/LP) creates |UP><LP| or |LP><UP| coherence states, leading to the oscillation dynamics.[9] Similar differences

can be seen for pulse sequence (LP/LP) and (LP/UP) (Figure 5c and d), in which coherence is created first, and either population or coherence states are created during t_2. Therefore, the clear distinction in dynamics shown in Figure 5, and the signature frequencies of 2D IR peaks in Figure 4 together verify that we can prepare either coherence or population states in the polariton systems, using an IR pulse shaper. We note that the population dynamics prepared by (UP/UP) and (LP/LP) exhibit different relaxation behaviors, which implies different distinguishable population relaxations when UP or LP is pumped[16], subjecting further investigation.

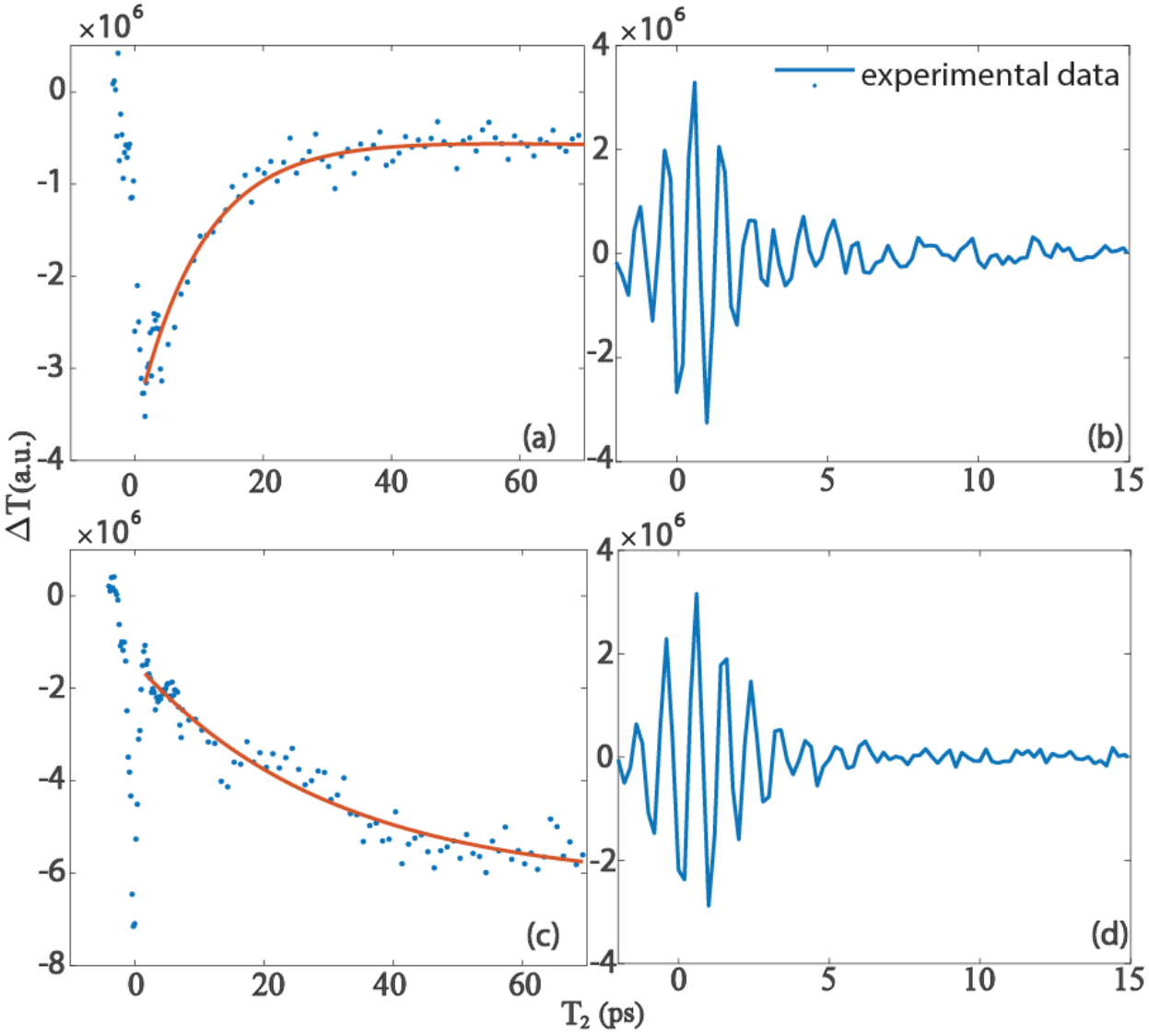

Figure 5 Dynamics of populations (a and c) and coherences (b and d) of polaritons pumped by (a) (UP/UP) (b) (UP/LP) (c) (LP/LP) (d) (LP/UP) tailored pump pulses. The intensity of the peak is obtained by the integration of the intensity of pixels of the dashed box in Figure 4. The lines in a and c are for eye guidance.

Discussion and Conclusion

The 2D IR spectrums and dynamic traces reproduce all the features expected from the quantum pathways excited by tailored pump pulse sequences. Thus, it verifies that we can selectively prepare desired quantum pathways. The sum of 2D IR spectra from four tailored pulse sequences reproduces the features of 2D IR using broadband pump pulses. Therefore, the tailored pulse sequence captures the nature of polariton interactions and dynamics well with quantum pathway specificity. A shaped probe pulse can provide further disentanglement of Feynman diagrams and prepare even more specific quantum states and pathways[27].

In summary, by using a two-level coherent quantum system formed by vibrational polariton as a toy model, we demonstrate the possibility to prepare arbitrary quantum states in polaritons. The experimental capability of preparing specific quantum states is useful to avoid unwanted interactions between states. It is also important to distinguish certain dynamics that cannot be separated by mathematical treatments. The coherent nature of molecular polaritons grants the system potential for quantum simulation/computing platforms[28–30], as well as understanding the role of coherence in energy transport processes in natural and artificial light-harvesting systems[31–35]. The presented result lays a foundation to prepare arbitrary quantum states in the polariton systems, i.e. to create |UP>+i|LP> states that is 90 degrees rotated from either |UP> or |LP> states.

Method

Molecule–Polariton Preparation and 2D IR Spectrometer. The $W(CO)_6$ (Sigma-Aldrich)/cavity system is prepared in an IR spectral cell (Harrick) containing saturated $W(CO)_6$/hexane solution and two dielectric CaF_2 mirrors with 96% reflectivity separated by a 25-μm spacer. The spectrometer follows the pulse shaper-enabled pump-probe design[25]. In the 2D IR spectrometer, three IR pulses interact with a sample sequentially to create two vibrational coherences. First, we scan t_1 to characterize the first coherence. Following, the second coherence introduces a macroscopic polarization which subsequently emits a third-order IR signal. This signal is self-heterodyned and detected in the frequency domain. To display 2D IR spectra, the FID in t_1 is numerically Fourier transformed.

AOM Pulse shaper. In our 2D IR experiments, the pulse shaper is used to turn the single incoming Gaussian pulse into two pulses with controllable time separation, phase and pulse shape. By taking the Fourier transform of this double pulse into the frequency domain, we obtain the amplitude and phase of each IR frequency. We can program the AWG to produce an RF signal that generates the acoustic wave needed to set the amplitude and phase of each IR frequency diffracted by the AOM such that a double pulse emerges with separation t_1.

Acknowledgment

The authors acknowledge Garret Wiesehan's help with the manuscript. W.X. thanks the NSF CAREER Award. Z.Y. is supported by DMR-1848215 and B. X. is supported by Roger Tsien Fellowship from the Department of Chemistry and Biochemistry at UCSD.

Reference

(1) Long, J. P.; Simpkins, B. S. Coherent Coupling between a Molecular Vibration and Fabry−Perot Optical Cavity to Give Hybridized States in the Strong Coupling Limit. *ACS Photonics* **2015**, *2*, 29. https://doi.org/10.1021/ph5003347.

(2) Shalabney, A.; George, J.; Hutchison, J.; Pupillo, G.; Genet, C.; Ebbesen, T. W. Coherent

Coupling of Molecular Resonators with a Microcavity Mode. *Nat. Commun.* **2015**, *6*. https://doi.org/10.1038/ncomms6981.

(3) Ebbesen, T. W. Hybrid Light-Matter States in a Molecular and Material Science Perspective. *Accounts of Chemical Research*. American Chemical Society November 15, 2016, pp 2403–2412. https://doi.org/10.1021/acs.accounts.6b00295.

(4) F. Ribeiro, R.; Dunkelberger, A. D.; Xiang, B.; Xiong, W.; Simpkins, B. S.; Owrutsky, J. C.; Yuen-Zhou, J. Theory for Nonlinear Spectroscopy of Vibrational Polaritons. *J. Phys. Chem. Lett.* **2018**, *9* (13), 3766–3771. https://doi.org/10.1021/acs.jpclett.8b01176.

(5) Saurabh, P.; Mukamel, S. Two-Dimensional Infrared Spectroscopy of Vibrational Polaritons of Molecules in an Optical Cavity. *J. Chem. Phys.* **2016**, *144* (12). https://doi.org/10.1063/1.4944492.

(6) Dunkelberger, A. D.; Spann, B. T.; Fears, K. P.; Simpkins, B. S.; Owrutsky, J. C. Modified Relaxation Dynamics and Coherent Energy Exchange in Coupled Vibration-Cavity Polaritons. *Nat. Commun.* **2016**, *7*. https://doi.org/10.1038/ncomms13504.

(7) Munkhbat, B.; Baranov, D. G.; Stührenberg, M.; Wersäll, M.; Bisht, A.; Shegai, T. Self-Hybridized Exciton-Polaritons in Multilayers of Transition Metal Dichalcogenides for Efficient Light Absorption. *ACS Photonics* **2019**, *6* (1), 139–147. https://doi.org/10.1021/acsphotonics.8b01194.

(8) Sun, Z.; Gu, J.; Ghazaryan, A.; Shotan, Z.; Considine, C. R.; Dollar, M.; Chakraborty, B.; Liu, X.; Ghaemi, P.; Kéna-Cohen, S.; et al. Optical Control of Roomerature Valley Polaritons. *Nat. Photonics* **2017**, *11* (8), 491–496.

https://doi.org/10.1038/nphoton.2017.121.

(9) Xiang, B.; Ribeiro, R. F.; Li, Y.; Dunkelberger, A. D.; Simpkins, B. B.; Yuen-Zhou, J.; Xiong, W. Manipulating Optical Nonlinearities of Molecular Polaritons by Delocalization. *Sci. Adv.* **2019**, *5* (9). https://doi.org/10.1126/sciadv.aax5196.

(10) Thomas, A.; Lethuillier-Karl, L.; Nagarajan, K.; Vergauwe, R. M. A.; George, J.; Chervy, T.; Shalabney, A.; Devaux, E.; Genet, C.; Moran, J.; et al. Tilting a Ground-State Reactivity Landscape by Vibrational Strong Coupling. *Science (80-.).* **2019**, *363* (6427), 615–619. https://doi.org/10.1126/science.aau7742.

(11) Hutchison, J. A.; Schwartz, T.; Genet, C.; Devaux, E.; Ebbesen, T. W. Modifying Chemical Landscapes by Coupling to Vacuum Fields. *Angew. Chemie Int. Ed.* **2012**, *51* (7), 1592–1596. https://doi.org/10.1002/anie.201107033.

(12) Thomas, A.; George, J.; Shalabney, A.; Dryzhakov, M.; Varma, S. J.; Moran, J.; Chervy, T.; Zhong, X.; Devaux, E.; Genet, C.; et al. Ground-State Chemical Reactivity under Vibrational Coupling to the Vacuum Electromagnetic Field. *Angew. Chemie Int. Ed.* **2016**, *55* (38), 11462–11466. https://doi.org/10.1002/anie.201605504.

(13) Vergauwe, R. M. A.; Thomas, A.; Nagarajan, K.; Shalabney, A.; George, J.; Chervy, T.; Seidel, M.; Devaux, E.; Torbeev, V.; Ebbesen, T. W. Modification of Enzyme Activity by Vibrational Strong Coupling of Water. *Angew. Chemie Int. Ed.* **2019**, *58* (43), 15324–15328. https://doi.org/10.1002/anie.201908876.

(14) Lather, J.; Bhatt, P.; Thomas, A.; Ebbesen, T. W.; George, J. Cavity Catalysis by Cooperative Vibrational Strong Coupling of Reactant and Solvent Molecules. *Angew.*

Chemie Int. Ed. **2019**, *58* (31), 10635–10638. https://doi.org/10.1002/anie.201905407.

(15) Xiang, B.; Ribeiro, R. F.; Dunkelberger, A. D.; Wang, J.; Li, Y.; Simpkins, B. S.; Owrutsky, J. C.; Yuen-Zhou, J.; Xiong, W. Two-Dimensional Infrared Spectroscopy of Vibrational Polaritons. *Proc. Natl. Acad. Sci. U. S. A.* **2018**, *115* (19), 4845–4850. https://doi.org/10.1073/pnas.1722063115.

(16) Xiang, B.; Ribeiro, R. F.; Chen, L.; Wang, J.; Du, M.; Yuen-Zhou, J.; Xiong, W. State-Selective Polariton to Dark State Relaxation Dynamics. *J. Phys. Chem. A* **2019**, *123* (28), 5918–5927. https://doi.org/10.1021/acs.jpca.9b04601.

(17) Wang, J.; Xiang, B.; Xiong, W. Ultrafast Intercavity Nonlinear Couplings between Polaritons. **2019**.

(18) Dunkelberger, A. D.; Davidson, R. B.; Ahn, W.; Simpkins, B. S.; Owrutsky, J. C. Ultrafast Transmission Modulation and Recovery via Vibrational Strong Coupling. *J. Phys. Chem. A* **2018**, *122* (4), 965–971. https://doi.org/10.1021/acs.jpca.7b10299.

(19) Chuntonov, L. 2D-IR Spectroscopy of Hydrogen-Bond-Mediated Vibrational Excitation Transfer. *Phys. Chem. Chem. Phys.* **2016**, *18* (20), 13852–13860. https://doi.org/10.1039/c6cp01640e.

(20) Ramakers, L. A. I.; Hithell, G.; May, J. J.; Greetham, G. M.; Donaldson, P. M.; Towrie, M.; Parker, A. W.; Burley, G. A.; Hunt, N. T. 2D-IR Spectroscopy Shows That Optimized DNA Minor Groove Binding of Hoechst33258 Follows an Induced Fit Model. *J. Phys. Chem. B* **2017**, *121* (6), 1295–1303. https://doi.org/10.1021/acs.jpcb.7b00345.

(21) Mackin, R. T.; Cohn, B.; Engelman, B.; Goldner, A.; Rubtsov, I. V.; Chuntonov, L.

Plasmonic Trimers for Dual-Frequency Surface-Enhanced Two-Dimensional Infrared Spectroscopy. *J. Phys. Chem. C* **2019**, *123* (40), 24731–24739. https://doi.org/10.1021/acs.jpcc.9b07045.

(22) Li, Y.; Wang, J.; Clark, M. L.; Kubiak, C. P.; Xiong, W. Characterizing Interstate Vibrational Coherent Dynamics of Surface Adsorbed Catalysts by Fourth-Order 3D SFG Spectroscopy. *Chem. Phys. Lett.* **2016**, *650*, 1–6. https://doi.org/10.1016/j.cplett.2016.02.031.

(23) Shim, S.-H.; Strasfeld, D. B.; Zanni, M. T. Generation and Characterization of Phase and Amplitude Shaped Femtosecond Mid-IR Pulses. *Opt. Express* **2006**, *14* (26), 13120. https://doi.org/10.1364/oe.14.013120.

(24) Shim, S.-H.; Strasfeld, D. B.; Fulmer, E. C.; Zanni, M. T. Femtosecond Pulse Shaping Directly in the Mid-IR Using Acousto-Optic Modulation. *Opt. Lett.* **2006**, *31* (6), 838. https://doi.org/10.1364/ol.31.000838.

(25) Shim, S. H.; Zanni, M. T. How to Turn Your Pump-Probe Instrument into a Multidimensional Spectrometer: 2D IR and Vis Spectroscopies via Pulse Shaping. *Physical Chemistry Chemical Physics*. 2009, pp 748–761. https://doi.org/10.1039/b813817f.

(26) Mukamel, S. *Principles of Nonlinear Optical Spectroscopy (Oxford Series on Optical and Imaging Sciences)*, New editio.; Oxford University Press, USA, 1999.

(27) Middleton, C. T.; Strasfeld, D. B.; Zanni, M. T. Polarization Shaping in the Mid-IR and Polarization-Based Balanced Heterodyne Detection with Application to 2D IR Spectroscopy. *Opt. Express* **2009**, *17* (17), 14526. https://doi.org/10.1364/oe.17.014526.

(28) Ladd, T. D.; Jelezko, F.; Laflamme, R.; Nakamura, Y.; Monroe, C.; O'Brien, J. L. Quantum Computers. *Nature*. 2010, pp 45–53. https://doi.org/10.1038/nature08812.

(29) Reiserer, A.; Rempe, G. Cavity-Based Quantum Networks with Single Atoms and Optical Photons. *Rev. Mod. Phys.* **2015**, *87* (4), 1379–1418. https://doi.org/10.1103/RevModPhys.87.1379.

(30) Hacker, B.; Welte, S.; Rempe, G.; Ritter, S. A Photon-Photon Quantum Gate Based on a Single Atom in an Optical Resonator. *Nature* **2016**, *536* (7615), 193–196. https://doi.org/10.1038/nature18592.

(31) Vasa, P.; Lienau, C. Strong Light-Matter Interaction in Quantum Emitter/Metal Hybrid Nanostructures. *ACS Photonics*. American Chemical Society January 17, 2018, pp 2–23. https://doi.org/10.1021/acsphotonics.7b00650.

(32) Ishizaki, A.; Fleming, G. R. Quantum Coherence in Photosynthetic Light Harvesting. *Annu. Rev. Condens. Matter Phys.* **2012**, *3* (1), 333–361. https://doi.org/10.1146/annurev-conmatphys-020911-125126.

(33) Cheng, Y.-C.; Fleming, G. R. Dynamics of Light Harvesting in Photosynthesis. *Annu. Rev. Phys. Chem.* **2009**, *60* (1), 241–262. https://doi.org/10.1146/annurev.physchem.040808.090259.

(34) Dong, S.; Trivedi, D.; Chakrabortty, S.; Kobayashi, T.; Chan, Y.; Prezhdo, O. V.; Loh, Z. H. Observation of an Excitonic Quantum Coherence in CdSe Nanocrystals. *Nano Lett.* **2015**, *15* (10), 6875–6882. https://doi.org/10.1021/acs.nanolett.5b02786.

(35) Hildner, R.; Brinks, D.; Van Hulst, N. F. Femtosecond Coherence and Quantum Control of

Single Molecules at Room Temperature. *Nat. Phys.* **2010**. https://doi.org/10.1038/NPHYS1858.